Anal. Chem. **2010,** *82,* 9455–9460

Lectin-Based Biosensor Strategy for Electrochemical Assay of Glycan Expression on Living Cancer Cells

Xinai Zhang,[†] Yingqiao Teng,[†] Ying Fu,[†] Lili Xu,[†] Shengping Zhang,[‡] Bei He,[‡] Chuangui Wang,*[,‡] and Wen Zhang*[,†]

Department of Chemistry, East China Normal University, Shanghai 200062, People's Republic of China, and Institute of Biomedical Sciences, College of Life Science, East China Normal University, Shanghai 200241, People's Republic of China

In this article, we report a novel lectin-based biosensor for electrochemical assay of cancer-associated glycosylation by comparative study of mannose and sialic acid expression on normal and cancer cells derived from human lung, liver, and prostate. Using a sandwich format, high sensitivity and selectivity were achieved by combining the lectin-based biosensor with the {lectin−Au−Th} bioconjugates featuring lectin and thionine (Th) labels linked to gold nanoparticles (AuNPs) for signal amplification. The proposed strategy demonstrated that mannose exhibited high expression levels in both normal and cancer cells, while sialic acid was more abundant in cancer cells as compared to normal ones. The results were in good agreement with those from fluorescent microscopy studies. The differences in the two glycan expression indicated that sialic acid could serve as a potential biomarker for early cancer detection. The lectin-based biosensor was also successfully used to quantify cancer cells and evaluate the average amount of sialic acid on single cell surface, which could supply significant information on glycan functions in cancer progression. Overall, the lectin-based electrochemical biosensor provides an effective pathway to analyze glycan expression on living cells and may greatly facilitate the medical diagnosis and treatment in early process of cancer.

Protein glycosylation is one of the most abundant and structurally diverse post-translational modifications in eukaryotic and prokaryotic organisms.[1,2] Glycoproteins on cell surface play crucial roles in a wide variety of biological processes, including cell growth and differentiation, cell−cell communication, and immune response modulation.[3,4] Alterations of glycan expression levels on glycoproteins have been shown to be associated with many diseases, such as diabetes, Alzheimer's disease, immune deficiencies, and especially cancers.[5−7] For example, the overall levels of fucose are much higher in ovarian and pancreatic cancer cells as compared to their corresponding normal controls.[8] α-GalNAc is expressed at a high level in breast tumorigenic MDA-MB-231 cells, while it is not expressed in normal MCF-10A cells.[9] Sialic acid expression has been found to be significantly elevated in colorectal cancer cells as compared to normal ones.[10] All these investigations indicate that the expression levels of glycans on glycoproteins can be used as therapeutic targets or clinical biomarkers for diagnosis of various cancers.[11] In recent years, many researchers have concentrated on the study of mannose and sialic acid, which are two important components of glycans correlated with glycosylation.[12−14] Mannose is the core structure of glycans on membrane glycoproteins, and the variation of its expression levels is observed in the course of tumorigenesis, brain aging, and differentiation.[15] Sialic acid is an important regulator of cellular and molecular interactions, and its overexpression on cell surface has been thought to be a characteristic feature associated with malignant properties.[16,17] Therefore, the comparative studies of the expression levels of mannose and sialic acid on normal and cancer cells might aid in the understanding of their roles in cancer development and help improve cancer diagnosis, prognosis, and treatment.

Up to now, a variety of methods have been used for glycan analysis such as mass spectrometry, nuclear magnetic resonance,

* To whom correspondence should be addressed. Phone: +86-21-62233509. Fax: +86-21-62232627. E-mail: wzhang@chem.ecnu.edu.cn.

[†] Department of Chemistry.

[‡] Institute of Biomedical Sciences, College of Life Science.

(1) Tian, Y.; Zhou, Y.; Elliott, S.; Aebersold, R.; Zhang, H. *Nat. Protoc.* **2007**, *2*, 334–339.
(2) Dwek, R. A. *Science* **1995**, *269*, 1234–1235.
(3) Varki, A. *Nature* **2007**, *446*, 1023–1029.
(4) Ohtsubo, K.; Marth, J. D. *Cell* **2006**, *126*, 855–867.
(5) Dube, D. H.; Bertozzi, C. R. *Nat. Rev. Drug Discovery* **2005**, *4*, 477–488.
(6) Matsumoto, A.; Sato, N.; Kataoka, K.; Miyahara, Y. *J. Am. Chem. Soc.* **2009**, *131*, 12022–12023.
(7) Zhang, Y.; Go, E. P.; Desaire, H. *Anal. Chem.* **2008**, *80*, 3144–3158.
(8) Ang, I. L.; Poon, T. C. W.; Lai, P. B. S.; Chan, A. T. C.; Ngai, S.-M.; Hui, A. Y.; Johnson, P. J.; Sung, J. J. Y. *J. Proteome Res.* **2006**, *5*, 2691–2700.
(9) Chen, S.; Zheng, T.; Shortreed, M. R.; Alexander, C.; Smith, L. M. *Anal. Chem.* **2007**, *79*, 5698–5702.
(10) Qiu, Y.; Patwa, T. H.; Xu, L.; Shedden, K.; Misek, D. E.; Tuck, M.; Jin, G.; Ruffin, M. T.; Turgeon, D. K.; Synal, S.; Bresalier, R.; Marcon, N.; Brenner, D. E.; Lubman, D. M. *J. Proteome Res.* **2008**, *7*, 1693–1703.
(11) Matsuno, Y.; Saito, T.; Gotoh, M.; Narimatsu, H.; Kameyama, A. *Anal. Chem.* **2009**, *81*, 3816–3823.
(12) Hennet, T.; Chui, D.; Paulson, J. C.; Marth, J. D. *Proc. Natl. Acad. Sci. U.S.A.* **1998**, *95*, 4504–4509.
(13) Kaneko, Y.; Nimmerjahn, F.; Ravetch, J. V. *Science* **2006**, *313*, 670–673.
(14) Nakagawa, K.; Kitazume, S.; Oka, R.; Maruyama, K.; Saido, T. C.; Sato, Y.; Endo, T.; Hashimoto, Y. *J. Neurochem.* **2006**, *96*, 924–933.
(15) Kubota, K.; Sato, Y.; Suzuki, Y.; Goto-Inoue, N.; Toda, T.; Suzuki, M.; Hisanaga, S.; Suzuki, A.; Endo, T. *Anal. Chem.* **2008**, *80*, 3693–3698.
(16) Alley, W. R., Jr.; Novotny, M. V. *J. Proteome Res.* **2010**, *9*, 3062–3072.
(17) Qiu, R.; Regnier, F. E. *Anal. Chem.* **2005**, *77*, 7225–7231.

10.1021/ac102132p
Published on Web 10/18/2010

and high-performance liquid chromatography.[18] Although those approaches can reveal molecular details, they require expensive equipment, much time for sample preparation, and are not amenable to living cell interrogation due to their destructivity.[19] Recently, electrochemical biosensors, typically based on glycans or ligands labeled with electroactive species to generate corresponding electrochemical signals, have attracted considerable interest in glycan assay[20−24] because of their simplicity, rapid response, and potential ability for real-time and on-site analysis.[25] To improve the sensitivity and selectivity of the biosensors, several methods have been developed by exploiting signal amplification strategies and new ligands. At present, the application of nanomaterials such as nanotubes, nanoparticles, and nanowires in the biosensor fabrication is one of the most popular techniques for their numerous signal amplifications and excellent electrocatalytic effects.[26,27] Regarding selectivity, the antibody-based biosensors, relying on the specific glycan-binding antibodies, have been extensively used to detect glycans.[28] However, the utilization of the antibody-based biosensors might be hindered by either high cost or relatively poor stability of antibodies.[29] Alternatively, lectins, which are structurally diverse proteins and exhibit highly specific binding affinity for glycans, provide an excellent candidate in biosensor design due to their unique merits such as ease of production and labeling, and stability during long-time storage.[30] Recent studies have described the use of lectins in analyzing oligosaccharide residues present on glycoproteins and indicated lectins as valuable tools for the structural and functional investigations of complex carbohydrates.[31]

Herein, we reported a lectin-based electrochemical biosensor for comparative study of the mannose and sialic acid expression levels in normal and cancer cells derived from human lung, liver, and prostate. Two lectins, concanavalin A (Con A) and *Sambucus nigra* agglutinin (SNA), were used to design the Con A-based and SNA-based biosensors that are specific for mannose and sialic acid, respectively.[9] In the case of the electrochemical assay, the biosensor was constructed by using gold nanoparticles/multiwalled carbon nanotubes (AuNP/MWNT) composite film as a substrate, which provided an effective matrix for the immobilization of lectins holding high stability and bioactivity. The sandwich-type system was formed by specific recognition of the biosensor surface-confined lectins to glycans on cell surface, followed by the attachment of the {lectin−Au−Th} bioconjugates featuring lectin and thionine (Th) labels linked to AuNPs. The analysis of mannose and sialic acid on cell surface was performed by electrochemical detection of Th in the bound bioconjugates on the biosensor. The results indicated that mannose displayed high expression levels in both normal and cancer cells, while sialic acid exhibited enhanced expression in cancer cells as compared to normal ones. The mannose and sialic acid expression status on living cell surface detected by the biosensor were in good agreement with the results from fluorescent microscopy studies. These differences in the two glycan expression demonstrated that sialic acid could serve as a potential biomarker for human lung, liver, and prostate cancer. Moreover, the electrochemical biosensor was also successfully applied to quantify cancer cells and evaluate the average amount of sialic acid on single cell surface. The proposed strategy facilitated highly sensitive and selective detection of glycans on living cell surface and offered great promise for the study of changes occurring in the process of cancer progression.

EXPERIMENTAL SECTION

Preparation of the {Lectin−Au−Th} Bioconjugates. Briefly, gold nanoparticles (AuNPs) were first prepared by the reduction of $HAuCl_4$ with trisodium citrate (see the Supporting Information).[32] Next, 30 mL of AuNPs solution was mixed with 6.0 mL of saturated thionine (Th) solution in water and stirred effectively for 24 h.[33] The resulting solution was centrifuged at 15 000*g* for 10 min to obtain the precipitate of Th-coated AuNPs. The precipitate was washed several times with water and redispersed in 4.0 mL of PBS. Last, the {lectin−Au−Th} bioconjugates were fabricated by addition of 50 μL of lectins (concanavalin A, Con A or *Sambucus nigra* agglutinin, SNA, 25 mg/mL) to the Th-coated AuNPs. After incubation for 4 h at 25 °C under shaking, the bioconjugates were isolated by centrifugation at 5000*g* for 12 min to remove the nonconjugated lectins and byproduct. Tris-HCl buffer and phosphate buffer saline (PBS, pH 7.4) were added to the prepared {Con A−Au−Th} and {SNA−Au−Th} bioconjugates to form homogeneous dispersions, respectively. The obtained bioconjugates solution was stored in a refrigerator at 4 °C.

Fabrication of the Lectin-Based Biosensor. Glass carbon working electrode (GCE, $\Phi = 3$ mm) was used to fabricate the lectin-based biosensor. Prior to surface modification, the electrode was polished with 0.05 μm alumina followed by successive sonication in acetone, HNO_3 (1:1, v/v), NaOH (50%, w/w), and pure water. Afterward, the clean GCE surface was modified by casting 10 μL of multiwalled carbon nanotubes (MWNTs, $\varphi = 10-30$ nm) in *N*,*N*-dimethylformamide (DMF, 0.10 mg/mL) and dried under infrared lamp. AuNPs were electrodeposited on the MWNT-modified GCE via multipotential step from +1.055 to −0.045 V (vs SCE) for 15 s in 0.50 M H_2SO_4 solution containing 0.10 mM $HAuCl_4$.[34] The AuNP/MWNT-modified GCE was incubated with thioglycolic acid (TGA, 25 mM) in ethanol for 24 h at room temperature (RT). The

(18) Szymanski, C. M.; St. Michael, F.; Jarrell, H. C.; Li, J. J.; Gilbert, M.; Larocque, S.; Vinogradov, E.; Brisson, J. R. *J. Biol. Chem.* **2003**, *278*, 24509–24520.
(19) Pilobello, K. T.; Mahal, L. K. *Curr. Opin. Chem. Biol.* **2007**, *11*, 300–305.
(20) Ertl, P.; Mikkelsen, S. R. *Anal. Chem.* **2001**, *73*, 4241–4248.
(21) Dai, Z.; Kawde, A.-N.; Xiang, Y.; La Belle, J. T.; Gerlach, J. Q.; Bhavanandan, V. P.; Joshi, L.; Wang, J. *J. Am. Chem. Soc.* **2006**, *128*, 10018–10019.
(22) Cheng, W.; Ding, L.; Ding, S. J.; Yin, Y. B.; Ju, H. X. *Angew. Chem., Int. Ed.* **2009**, *48*, 6465–6468.
(23) Ding, L.; Cheng, W.; Wang, X. J.; Ding, S. J.; Ju, H. X. *J. Am. Chem. Soc.* **2008**, *130*, 7224–7225.
(24) Xue, Y. D.; Ding, L.; Lei, J. P.; Yan, F.; Ju, H. X. *Anal. Chem.* **2010**, *82*, 7112–7118.
(25) Zhang, S.; Xia, J.; Li, X. *Anal. Chem.* **2008**, *80*, 8382–8388.
(26) Yu, X.; Munge, B.; Patel, V.; Jensen, G.; Bhirde, A.; Gong, J. D.; Kim, S. N.; Gillespie, J.; Gutkind, J. S.; Papadimitrakopoulos, F.; Rusling, J. F. *J. Am. Chem. Soc.* **2006**, *128*, 11199–11205.
(27) Lu, X. M.; Tnan, H. Y.; Korgel, B. A. *Chem.-Eur. J.* **2008**, *14*, 1584–1591.
(28) Willats, W. G. T.; Rasmussen, S. E.; Kristensen, T.; Mikkelsen, J. D.; Knox, J. P. *Proteomics* **2002**, *2*, 1666–1671.
(29) Xu, H.; Mao, X.; Zeng, Q.; Wang, S.; Kawde, A.-N.; Liu, G. *Anal. Chem.* **2009**, *81*, 669–675.
(30) Nilsson, C. L. *Anal. Chem.* **2003**, *75*, 348A–353A.
(31) Jelinek, R.; Kolusheva, S. *Chem. Rev.* **2004**, *104*, 5987–6015.
(32) Grabar, K. C.; Freeman, R. G.; Hommer, M. B.; Natan, M. J. *Anal. Chem.* **1995**, *67*, 735–43.
(33) Ding, Y.; Zhang, X.; Liu, X.; Guo, R. *Langmuir* **2006**, *22*, 2292–2298.
(34) Dai, X.; Nekrassova, O.; Hyde, M. E.; Compton, R. G. *Anal. Chem.* **2004**, *76*, 5924–5929.

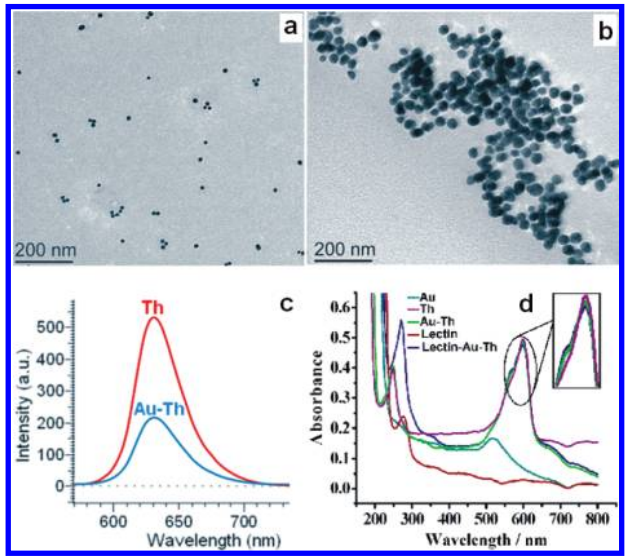

Figure 1. TEM images of AuNPs (a) and Th-coated AuNPs (b); (c) fluorescence emission spectra of Th (red line) and Th-coated AuNPs (blue line); (d) UV−vis absorption spectra of AuNPs, Th, Th-coated AuNPs, lectins, and the {lectin−Au−Th} bioconjugates.

electrode surface was rinsed with ethanol and PBS, and then dried with nitrogen. Subsequently, 10 μL of 400 mM 1-ethyl-3-(3-dimethylaminopropyl) carbodiimide (EDC) and 100 mM *N*-hydroxysuccinimide (NHS) solution was cast on the electrode surface to activate carboxyl group of TGA for 1 h. The activated electrode was rinsed with PBS and incubated with 1.0 mg/mL Con A or SNA (the optimal lectin concentration that was investigated in Figure S-1, Supporting Information) for 50 min to prepare the Con A-based or SNA-based biosensor. The biosensor was treated with 1.0% BSA/PBS for 30 min to block the nonspecific binding.

Electrochemical Detection of Glycans on Cell Surface. After being rinsed and dried in nitrogen, the Con A-based and SNA-based biosensors were incubated with cell suspension at a certain concentration for 50 min at RT, and then washed with Tris-HCl buffer and PBS, respectively. Subsequently, 10 μL of {Con A−Au−Th} or {SNA−Au−Th} bioconjugates were dropped on the cell-captured electrode and incubated for 50 min. The resulting electrode was rinsed with water, and then immersed in HAc−NaAc buffer solution (pH 7.0) to detect the immobilized Th with differential pulse voltammetry (DPV) from 0 to −0.70 V (vs SCE).

RESULTS AND DISCUSSION

Characterization of the {Lectin−Au−Th} Bioconjugates. The TEM images of AuNPs before and after the addition of Th are displayed in Figure 1. As shown in Figure 1a, the spherical AuNPs were found as dispersed particles with an average diameter of 18 nm. The conjugation of Th on AuNPs led to a larger particle diameter (Figure 1b). The Th-coated AuNPs exhibited small clusters due to surface charge neutralization of the cationic Th molecules and the negative citrate-protected AuNPs.[33] The observed clusters were well separated and could be distinguished as individual in TEM micrographs. The fluorescence emission spectra of Th (red line) and the Th-coated AuNPs (blue line) are shown in Figure 1c. Significantly, both spectra exhibited a maximum emission peak around 630 nm when excited at 535 nm. As compared to Th, the fluorescence intensity of the Th-coated AuNPs decreased greatly. The decreased fluorescence indicates that a large fraction of excited Th molecules are quenched by AuNPs, which is attributed to the electronic interaction between Th molecules and AuNPs.

UV−vis absorption spectrometry was used to investigate the preparation process of the {lectin−Au−Th} bioconjugates (Figure 1d). Apparently, AuNPs displayed an absorption peak at 520 nm. Th exhibited two characteristic peaks at 600 and 565 nm, which were assigned to monomer and H-dimer forms, respectively. When Th was attached to AuNPs, the intensity of 600 nm decreased and that of 565 nm increased, indicating that AuNPs facilitated the transition of Th from monomer to H-dimer forms. The slightly blue-shifted peak position of 565 nm was probably due to the strong electronic coupling between Th molecules in the Th-coated AuNPs. When lectins were conjugated to the Th-coated AuNPs, a 268 nm absorption peak was observed, and the absorption wavelength was obviously less than that of pure lectins. The reason was attributed to the interoverlapping of 250 nm (for Th) and 276 nm (for lectins). The results suggested that the {lectin−Au−Th} bioconjugates could be fabricated on the basis of the conjugation of lectins to the Th-coated AuNPs.

Additionally, the specific recognition of the {lectin−Au−Th} bioconjugates to cell surface glycans was verified by a blocking experiment (Figure S-2 in the Supporting Information).

Characterization of the Lectin-Based Biosensor. Figure 2 shows the SEM images of GCE modified with MWNT, AuNP/MWNT, and lectin/AuNP/MWNT, respectively. Figure 2a exhibits that MWNTs were mostly in the form of small bundles or single tubes on GCE. As shown in Figure 2b, the well-dispersed AuNPs decorated uniformly on the walls of nanotubes. This uniform nanostructure provides an effective electrode surface for loading lectins and accelerating electron transfer. Figure 2c shows that lectins were well spread on the electrode surface. Because of the porous structure and the excellent properties of the AuNP/MWNT composite film, the nanostructure retained the bioactivity of lectins to produce attractive performances of the lectin-based biosensor. The electrochemical properties of the lectin-based biosensor after each assembly step were also studied by electrochemical impedance spectroscopy and cyclic voltammetry (Figure S-3 in the Supporting Information).

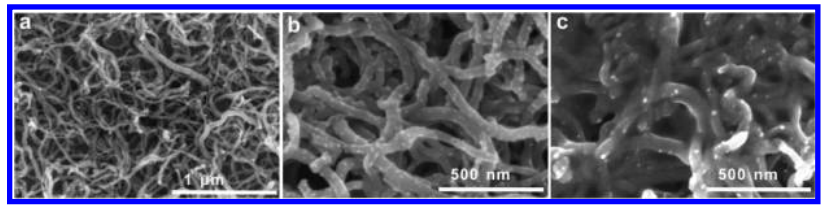

Figure 2. SEM images of (a) MWNT/GCE, (b) AuNP/MWNT/GCE, and (c) lectin/AuNP/MWNT/GCE.

Scheme 1. Schematic Illustration of the Lectin-Based Biosensor for Electrochemical Analysis of Glycan Expression on Living Cells

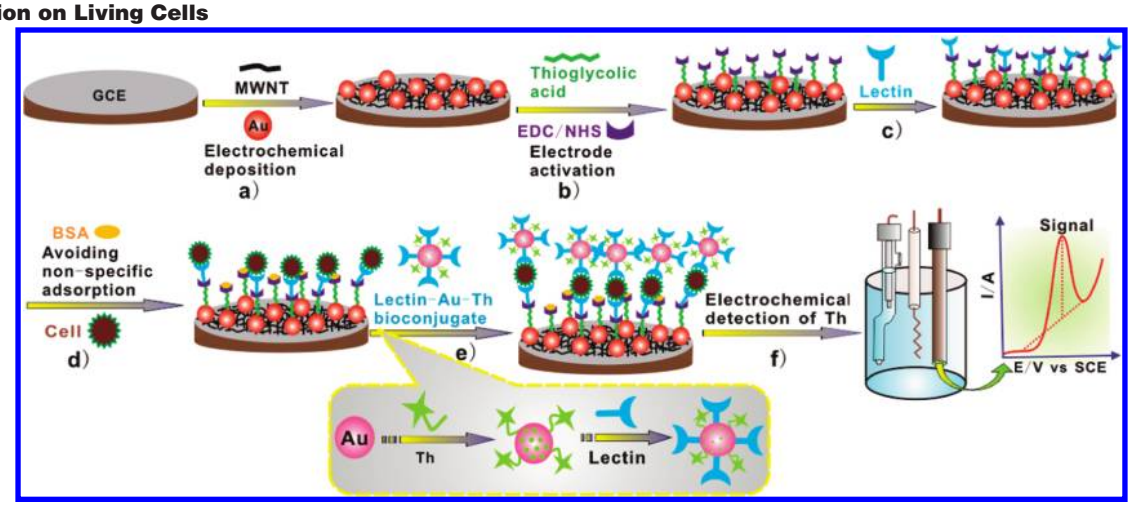

Mechanism of Electrochemical Strategy with the Lectin-Based Biosensor. The mechanism of electrochemical strategy with the lectin-based biosensor for the study of mannose and sialic acid on cell surface is illustrated in Scheme 1. In the preparation process of the lectin-based biosensor, the AuNP/MWNT composite film was employed as the substrate, which was designed by first introduction of MWNTs on GCE surface and then electrodeposition of AuNPs by multipotential step (Scheme 1a). Subsequently, TGA was assembled on the AuNP/MWNT/GCE surface through Au−S bond, and the carboxyl group of TGA was activated by using EDC/NHS (Scheme 1b), which introduced a high density of lectins (Scheme 1c). After further treated with BSA to block the nonspecific binding, the biosensor could effectively capture cells by the specific interaction between surface-confined lectins and glycans on cell surface (Scheme 1d), followed by the attachment of the {lectin−Au−Th} bioconjugates to form a sandwich-type system (Scheme 1e). The {lectin−Au−Th} bioconjugates were fabricated by exploiting the amplification effect of AuNPs for the mass loading of Th to achieve high sensitivity, in which lectins were used for recognition of cell surface glycans and Th served as electroactive species. The Th labels in the bound bioconjugates were recorded by electrochemical detection (Scheme 1f). Because Th was only present when lectins reacted with glycans on cell surface, the peak current reflected the expression levels of cell surface glycans and the amount of captured cells on the biosensor, providing a strategy for the analysis of glycan expression on living cells.

Enhancing Sensitivity in the Biosensor Using AuNP/MWNT/GCE as Substrate. To evaluate the analytical performance of the lectin-based biosensor, different substrates, including AuNP/GCE, MWNT/GCE, and AuNP/MWNT/GCE, were applied to the biosensor design for the detection of glycans on A549 cells (lung cancer cells). Figure 3A shows the DPV peak current on different Con A-based biosensors that were used to detect mannose expression on A549 (1.0×10^6 cells/mL). It was observed that the highest current was obtained on the AuNP/MWNT-modified GCE, which was attributed to the excellent electrocatalytic effects of the AuNP/MWNT composite film. As shown in Figure 3B, the Con A-based and SNA-based biosensors were also used for the analysis of mannose and sialic acid on A549 cells (1.0×10^4 and 1.0×10^6 cells/mL), respectively. The results confirmed that the lectin-based biosensor using AuNP/MWNT-modified GCE as a substrate has the capability of enhancing sensitivity. Therefore, the proposed biosensor could improve the detection limits and reduce the risk of false negative determination at low cell concentrations.

Electrochemical Analysis of Glycan Expression on Cell Surface. The Con A-based and SNA-based biosensors were applied to analyze mannose and sialic acid on different human normal and cancer cells, respectively. Figure 4A exhibits the DPV peak current on the Con A-based biosensor for evaluation of mannose expression on MRC-5 (lung normal cells), A549, and H1299 (cancer cells). As can be shown, a large peak current was obtained for the detection of mannose on these three kinds of cells. Figure 4B displays the peak current for the assay of sialic acid expression levels by using the SNA-based biosensor. Obvi-

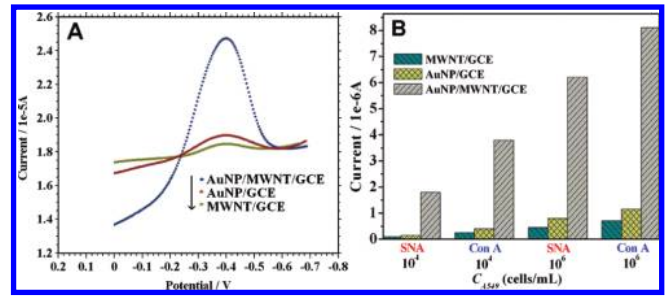

Figure 3. Comparison of DPV peak current on the lectin-based biosensors using AuNP/GCE, MWNT/GCE, and AuNP/MWNT/GCE as substrates. (A) Peak current on the Con A-based biosensors for A549 cell detection (1.0×10^6 cells/mL); (B) graphical representation of peak current on the Con A-based and SNA-based biosensors for A549 cell detection (1.0×10^4 and 1.0×10^6 cells/mL).

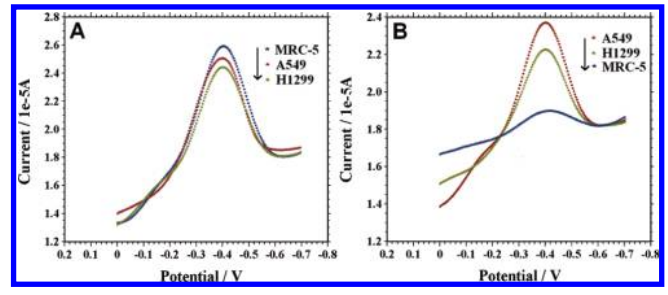

Figure 4. DPV peak current for the detection of mannose and sialic acid on MRC-5, A549, and H1299 cells using (A) the Con A-based biosensor and (B) the SNA-based biosensor, respectively.

Table 1. Assay Results of Cancer Cells with the SNA-Based Biosensor

cell	linear regression equation	linear range (cells/mL)	R	limit of detection (LOD, cells/mL)
A549	i_p (μA) = 1.43 lg c_{A549} − 2.40	3.0×10^4 to 3.0×10^7	0.993	7.0×10^3
H1299	i_p (μA) = 1.38 lg c_{H1299} − 3.36	3.0×10^5 to 3.0×10^8	0.991	8.0×10^4
95-D	i_p (μA) = 1.42 lg $c_{95\text{-}D}$ − 3.57	2.5×10^5 to 2.5×10^8	0.994	7.0×10^4
QGY-7701	i_p (μA) = 1.45 lg $c_{QGY\text{-}7701}$ − 3.91	3.6×10^5 to 3.6×10^8	0.993	1.1×10^5
QGY-7703	i_p (μA) = 0.86 lg $c_{QGY\text{-}7703}$ + 3.42	10 to 1.0×10^6	0.992	5.0
LNCaP	i_p (μA) = 1.24 lg c_{LNCaP} −2.35	2.0×10^5 to 5.0×10^8	0.995	5.0×10^4

ously, there was no considerable current observed in the presence of MRC-5 cells. Unlike MRC-5, A549 and H1299 induced strong response signal on the SNA-based biosensor. Table S-1 (Supporting Information) summarizes the peak current on the Con A-based and SNA-based biosensors for analysis of the expression of mannose and sialic acid on normal and cancer cells derived from human lung, liver, and prostate. The results demonstrated that mannose was commonly expressed on the selected cells, while sialic acid was more abundant in cancer cells than that in normal ones.

Quantitative Detection of Cancer Cells with the SNA-Based Biosensor. As is well-known, highly sensitive detection of cancer cells is extremely important for early cancer diagnosis, and thus greatly increases the chance for effective treatment.[35] In view of the above challenges, we used the SNA-based biosensor for the quantification of cancer cells on the basis of the specific recognition between SNA and sialic acid on cell surface. The peak current obtained with the lectin-based biosensor was proportional to the logarithmic value of cell concentration. Table 1 shows the results for the quantitative assay of cancer cells.

By comparing those cell-based biosensors reported in the literature,[36,37] we confirmed that the proposed biosensor exhibited good performances for the detection of cancer cells with wide linear ranges and low detection limits. The interesting results indicated that the electrochemical strategy could afford a simple and applicable way for the quantification of cancer cells, suggesting a potential application in cancer diagnosis.

Evaluation of Sialic Acid Expression on Cancer Cells. Sialic acid on cell surface has been implicated in aggressive cancer cell behavior, and its expression on living cells can provide essential information on cancer status progression.[38] Thus, it is important to evaluate the amount of sialic acid on single cell surface for understanding the roles of sialic acid in cancer development. For this purpose, a method was designed by first detecting sialic acid to obtain the standard curve using the SNA-based biosensor. As shown in Figure 5A, the DPV peak current (i_p) exhibited a linear relation with sialic acid concentration ($c_{\text{sialic acid}}$) in the range 0.5−5.0 μM ($R = 0.992$). The linear regression equation is

$$i_p\ (\mu\text{A}) = 0.19 c_{\text{sialic acid}}\ (\mu\text{M}) + 4.99 \qquad (1)$$

Under the same experimental conditions, the SNA-based biosensor was used for the detection of cancer cells at different concentrations. The peak current (i_p') versus A549 cell concentration (c_{A549}) showed linear relation in the range of 2.0×10^5 to 7.0×10^5 cells/mL ($R = 0.994$) (Figure 5B), and the equation is

$$i_p'\ (\mu\text{A}) = 1.30 \times 10^{-6} c_{A549} + 5.04 \qquad (2)$$

Meanwhile, the i_p' for A549 cell detection could be converted into the amount of sialic acid according to eq 1, which represented the expression level of sialic acid on A549 cells. Consequently, with the use of eqs 1 and 2, the amount of sialic acid on each cell surface ($n_{\text{sialic acid}}$) was calculated from the following equation:

$$n_{\text{sialic acid}} = \frac{(i_p - 4.99) \times 10^{-6} \times (6.02 \times 10^{23})}{(0.19 \times 10^3) \times c_{\text{cell}}} \qquad (3)$$

where c_{cell} was the concentration of cancer cells in cells/mL. Four parallel measurements gave the average amount of sialic acid on single cell surface to be 4.5×10^9 molecules for A549 cells. Using the same method, the sialic acid expression on the other cancer cells was also evaluated, and the obtained results are summarized in Table 2. Moreover, the control experiment was performed to detect the amount of sialic acid on each cell surface, which supported the proposed method (Figure S-4 in the Supporting Information).

Fluorescent Imaging of Glycan Expression on Cell Surface. The fluorescent analysis is one of the conventional methods to monitor molecules of biological importance in clinical laboratory.[39] We challenged the proposed biosensors with fluorescent images for the assay of mannose and sialic acid on normal and cancer cells derived from human lung, liver, and prostate. Both Fluorescein Con A and Fluorescein SNA were used as fluorescent

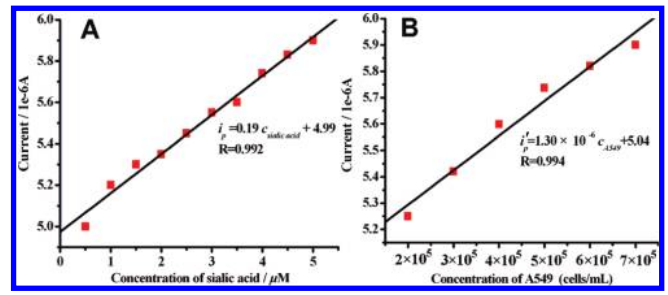

Figure 5. Linear calibration plots of peak current on the SNA-based biosensor versus concentrations of (A) sialic acid standard sample and (B) A549 cells in PBS.

(35) Zhang, J.-J.; Cheng, F.-F.; Zheng, T.-T.; Zhu, J.-J. *Anal. Chem.* **2010**, *82*, 3547–3555.
(36) Laczka, O.; Baldrich, E.; Muñoz, F. X.; del Campo, F. J. *Anal. Chem.* **2008**, *80*, 7239–7247.
(37) Pan, C. F.; Guo, M. L.; Nie, Z.; Xiao, X. L.; Yao, S. Z. *Electroanalysis* **2009**, *21*, 1321–1326.
(38) Chang, P. V.; Chen, X.; Smyrniotis, C.; Xenakis, A.; Hu, T.; Bertozzi, C. R.; Wu, P. *Angew. Chem., Int. Ed.* **2009**, *48*, 4030–4033.

Table 2. Assay Results of Sialic Acid Expression on Cancer Cells with the SNA-Based Biosensor

cell	linear regression equation	linear range (cells/mL)	R	amount of sialic acid on single cell surface (molecules)
A549	i_p' (μA) $= 1.30 \times 10^{-6} c_{A549} + 5.04$	2.0×10^5 to 7.0×10^5	0.994	4.5×10^9
H1299	i_p' (μA) $= 1.70 \times 10^{-7} c_{H1299} + 4.98$	2.0×10^6 to 4.0×10^6	0.993	5.3×10^8
95-D	i_p' (μA) $= 2.10 \times 10^{-7} c_{95\text{-}D} + 4.93$	1.5×10^6 to 4.0×10^6	0.995	5.9×10^8
QGY-7701	i_p' (μA) $= 1.60 \times 10^{-7} c_{QGY\text{-}7701} + 4.96$	3.0×10^6 to 5.0×10^6	0.992	4.8×10^8
QGY-7703	i_p' (μA) $= 8.07 \times 10^{-4} c_{QGY\text{-}7703} + 5.30$	2.0×10^2 to 8.0×10^2	0.995	5.0×10^{12}
LNCaP	i_p' (μA) $= 2.70 \times 10^{-7} c_{LNCaP} + 4.85$	1.0×10^6 to 4.0×10^6	0.996	6.4×10^8

signal-generating elements (via adducted fluorescein molecules) and recognition elements (via adducted Con A or SNA proteins). After Fluorescein Con A or Fluorescein SNA was incubated with cells on the slides, the stained samples were scanned to obtain fluorescent images. As shown in Figure S-5 (Supporting Information), the slides treated with Fluorescein Con A exhibited strong fluorescent signals in the regions of normal and cancer cells. When Fluorescein SNA was placed on the slides, fluorescent signals from cancer cells were stronger than those from normal ones. Additionally, the mean fluorescence intensity was obtained from the images of the corresponding lectin slides by the addition of different cells (Figure S-6 in the Supporting Information). On the basis of binding strength of Fluorescein Con A and Fluorescein SNA to cells, the variety of fluorescence intensity clearly showed the difference among the expression of mannose and sialic acid on cell surface.

The glycan expression status on cell surface obtained by fluorescent microscopy studies was consistent with the results from the lectin-based biosensors, and both demonstrated that mannose displayed common high expression levels in normal and cancer cells, while sialic acid exhibited enhanced expression on cancer cells as compared to normal controls. These differences in the two glycan expression indicated that sialic acid could serve as a potential biomarker for human lung, liver, and prostate cancer.

CONCLUSIONS

Glycans, mannose and sialic acid, are known to be functionally important and to have potential diagnostic value. This work developed a novel lectin-based electrochemical biosensor for highly sensitive and selective detection of cancer-associated glycosylation by comparative study of mannose and sialic acid expression on normal and cancer cells derived from human lung, liver, and prostate. Two lectins, Con A and SNA, which are, respectively, specific for mannose and sialic acid, were used to design the Con A-based and SNA-based biosensors for the analysis of glycans on cell surface. Our data showed that mannose exhibited high expression levels in both normal and cancer cells, while sialic acid was more abundant in cancer cells as compared to normal controls. These differences in the glycan expression on different cells indicated that sialic acid could serve as a potential biomarker for early cancer detection. The proposed biosensor was also successfully applied to quantify cancer cells and evaluate the average amount of sialic acid on single cell surface. The lectin-based biosensor could be expanded for other glycans by using a greater variety of lectins and thus provided a powerful tool for evaluating glycan expression on living cells and revealing glycan functions in underlying biological processes related to cancers.

(39) Bates, M.; Huang, B.; Dempsey, G. T.; Zhuang, X. *Science* **2007**, *317*, 1749–1753.

ACKNOWLEDGMENT

This work was supported by the National Natural Science Foundation of China (20775026, 21075041, 30772523), the Science and Technology Commission of Shanghai Municipality (1052 nm06500), the National Basic Research Program of China (2009CB918401), and the "Shu Guang Project" of the Shanghai Municipal Education Commission, People's Republic of China (05SG30).

SUPPORTING INFORMATION AVAILABLE

Additional information as noted in text. This material is available free of charge via the Internet at http://pubs.acs.org.

Received for review August 13, 2010. Accepted October 4, 2010.

AC102132P